Carbonates and Evaporites (2019) 34:1367–1379
https://doi.org/10.1007/s13146-018-0439-9

ORIGINAL ARTICLE

# Formation phases of carbonate cements and sedimentary environments in lower Jurassic sandstones of the Lenghu V tectonic belt, North Qaidam Basin, China

**Jiajia Guo[1,2] · Guoqiang Sun[1] · Weiming Liu[1,2]**

Accepted: 16 February 2018 / Published online: 5 March 2018
© Springer-Verlag GmbH Germany, part of Springer Nature 2018

**Abstract**
Based on petrography and geochemistry, formation phases of carbonate cements and their sedimentary–diagenetic environments in Jurassic clastic rocks from the Lenghu V tectonic belt are determined. The results demonstrate that studied successions are mainly dark gray or black mudstone with interbedded thin gray siltstone and a few greywacke layers. Sandstones are lithic and feldspathic lithic greywacke with high kaolinite content. Calcite and ferrocalcite are the main carbonate cements. The carbon isotope values($\delta^{13}C$) of the carbonate cements range from − 15.6 to 9.2‰ (average − 3.2‰) with a bimodal distribution. One peak is 4‰, which includes samples from the upper Xiaomeigou Formation (Fm) and the other one is − 12‰, which mainly represents the lower section. The oxygen isotope values($\delta^{18}O$) have a wide range from − 18.5 to − 8.3‰ (average − 13.31‰). Combined with microscopic observations, two phases of carbonate cements are distinguished according to their isotopic characteristics. The earlier carbonate cements are mainly calcite and ferrocalcite, and they were precipitated in eodiagenesis stage. The carbon source of calcite was inorganic, and ferrocalcite was mixed with carbon from methanogenesis. This mixture led to a positive bias in the $\delta^{13}C$ curve, which artificially inflated the paleosalinity. The later carbonate cements, formed in mesodiagenesis stage, were ferrocalcite. Decarboxylation of organic matters led to lower $\delta^{13}C$ values. The major and trace elements data show that Sr, Ba, Fe and Mn have weak correlation with Al, Ti. So, they are effective to interpret the sedimentary environment. The Sr/Ba ratio < 1 indicates fresh water environment, Sr/Ca, Sr/Cu and Fe/Mn ratios suggest humid climate, and V/(V + Ni) ratio shows suboxic–anoxic environment. The carbon and oxygen isotopes, together with elemental geochemistry, show that the climate during the Early Jurassic was warm and wet and the studied successions were deposited in fresh water. The variations in elemental ratio curves indicate that climate became wetter and warmer later in the Early Jurassic.

**Keywords** Carbon isotope · Oxygen isotope · Carbonate cements · Sedimentary environment · Qaidam Basin

## Introduction

Sedimentary environment is an important aspect of sedimentological research. There are many researches on paleosalinity and paleoclimate, which include the use of lithofacies and primary sedimentary structure (Lu et al. 1997; Yang et al. 2007), the application of specific clay mineral content (Xie et al. 2010; Tang et al. 2002; Zeng and Xia 1986), and the analysis of isotopic data, major and trace elements (Xiong and Xiao 2011; Wang et al. 2006). Each of these methods has its own advantages and limitations. For example, changes in paleoenvironment can be easily resolved by elemental geochemistry, but it is difficult to build up a uniform standard in different geological backgrounds.

In recent years, researches on diagenetic evolution and sedimentary–diagenetic environments in the light of isotopic data of carbonate cements have increased (Sun et al. 2015a, b; Yuan and Li 2011; Hu 2003). However, these researches have their limitations. Effectively integrated approaches are deficient.

✉ Guoqiang Sun
sguoqiang@lzb.ac.cn

[1] Key Laboratory of Petroleum Resources, Gansu Province/Key Laboratory of Petroleum Resources Research, Institute of Geology and Geophysics, Chinese Academy of Science, Lanzhou 730000, China

[2] University of Chinese Academy of Sciences, Beijing 100049, China

The Qaidam Basin is an important tectonic unit in China and hosts abundant oil and gas reserves; it is a petroleum system with Jurassic source rocks and Paleogene and Neogene reservoirs. The Lenghu V tectonic belt lies in the Shaikun faulting–subsiding subregion in the northern Qaidam Basin (Fig. 1). According to pollen and other (micro) fossil studies (Ma and Zhang 2005), the stratum from 3470 to 4666 m depth was deposited during early Jurassic; however, the lower limit of this section is under some debate, and based on some studies may be extended to 5200 m. Based on organic geochemical indices, evolution characteristics and formation/distribution sequences of authigenic minerals, 4200 m is the boundary of phases A and B of the middle diagenetic stage, and 4666 m represents the boundary between the middle and late diagenetic stages (Kou et al. 2005; Wang and Wang 2006). The sedimentological and paleontological aspects of these Jurassic successions in the northern Qaidam Basin was studied based on Yang et al. (2007). This study investigates the paleoenvironment and carbonate cementation by analyzing the clay minerals, carbon and oxygen isotopes of carbonate cements and the elemental geochemistry of the Xiaomeigou Formation (early Jurassic) in the Lenghu V tectonic belt.

## Materials and methods

The sedimentological data including thin section identification and X-ray diffraction were provided by the Exploratory Development Institute of Qinghai Petroleum Administration.

The samples in this paper are from the lower Jurassic successions of LK1 well in the Lenghu V tectonic belt. The recovered cores from the Xiaomeigou Fm compose of eight sections including 3482.1–3486.13 m, 3510–3521.92 m, 3536.15–3542.55 m, 3751.87–3756.77 m, 4235.1–4241.01 m, 4306.24–4321.93 m, 4377.5–4384.66 m, 4413.06–4418.58 m, and the total length of the recovered cores is 61 m. Before the sampling, careful descriptions and analysis regarding rock types, lithology and sedimentary structures were done. 34 sandstone and siltstone samples were collected to analyze the carbon and oxygen isotopes, 25 mudstone samples were collected to analyze the major and trace elements content. Mudstone samples were from three separate depths (3510–3544 m, 3752–3757 m and 4236–4241 m) approximately cover the Xiaomeigou Fm.

The sandstone samples were treated with 1% hydrochloric acid. Determination of carbonate cement types was based on the bubbling intensity (Sun et al. 2015a, b). After

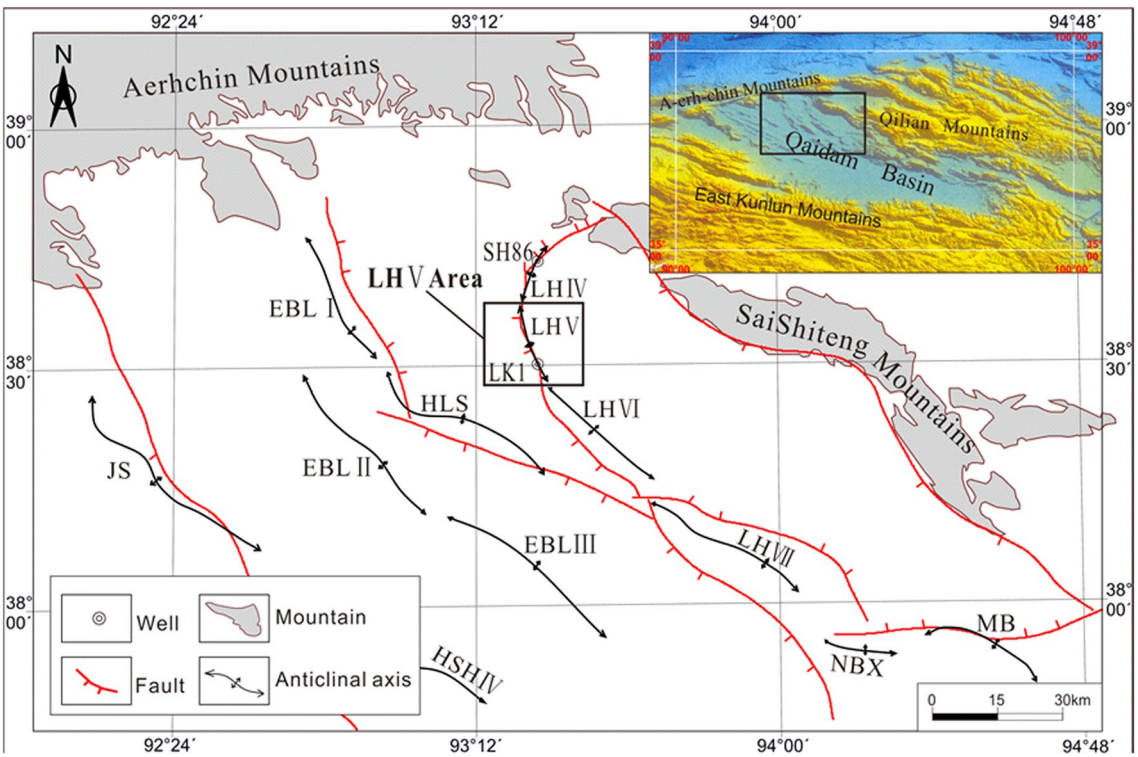


**Fig. 1** Characteristics of the structures in the northern edge of the Qaidam Basin. LHVI Lenghu VI, LHVII Lenghu VII, NBX Nanbaxian, MB Mabei, JLS Jiulongshan, JS Jianshan, HLS Hulushan, EBLI Eboliang I, EBLII Eboliang II, EBLIII Eboliang III, HSHIII Hongsanhan III, HSHIV Hongsanhan IV, YH Yau, TJNE Taijinaier, YKYWR Yikeyawuru

this preliminary determination, microscopic identification was used to choose samples with no clastic carbonates to insure carbon and oxygen isotope data are from carbonate cements (Wang et al. 2010). A MAT252 (ThermoFinnigan, Germany) stable isotope ratio mass spectrometer was used for the isotope analyses. After grinding, the powder was passed over a 100–200 mesh sieve. Sufficient quantities of 100% orthophosphoric acid were added to samples, and left to react at 90 °C. The $CO_2$ was measured by the mass spectrometer after drying. All carbon and oxygen isotope data are reported against the Pee Dee Belemnite (PDB) standard.

Before the elemental analysis, all mudstone samples were visually checked for alteration, mineralization and weathering under the microscope. Samples were grinded in a pollution-free environment and screened through a 200 mesh sieve, then baked in an oven for 3 h to remove moisture. Major elements (Na, Mg, Al, Si, P, K, Ca, Fe) were measured by fluorescence spectrometry (3080E3X, Rigaku), and trace elements (e.g., Ti, V, Cr, Mn, Ni, Cu) were examined by inductively coupled plasma-mass spectrometry (ICP-MS) with dissolved samples sealed by $HF+HNO_3$. These analyses were performed at the Key Laboratory of Petroleum Resources Research (Institute of Geology and Geophysics, Chinese Academy of Science).

## Sedimentary and petrological characteristics

### Characteristics of lower Jurassic of LK1 in North margin of Qaidam Basin

The Jurassic strata are deeply buried in the northern Qaidam Basin, generally lying deeper than 3000 m in the Lenghu V tectonic belt. The average thickness of the lower Jurassic deposits is 1193 m, and it is the main source rock in the northern Qaidam Basin. It comprises the Xiaomeigou Fm, which can be divided into two parts. The lakeshore facies developed in the upper part and mainly consist of dark gray and black mudstone with interbedded thin gray siltstone and greywacke layers. The braided river delta front facies are present in the lower part and the lithology is similar to the upper part, but with larger amounts of interbedded gray siltstone and greywacke layers. The transition zone between the two parts is the main coal-bearing series (Fig. 2). According to the point counting of about 200 prepared thin sections, the quartz content in clastic rocks is 10–55% (average 25%), feldspar is 5–28% (average 16.5%) and the detrital content is 10–80% (average 45.7%). The sandstone is mainly litharenite and feldspathic litharenite with small amounts of lithic arkose according to Folk's classification (Fig. 3). Plagioclase is the main composition of the feldspathic debris, followed

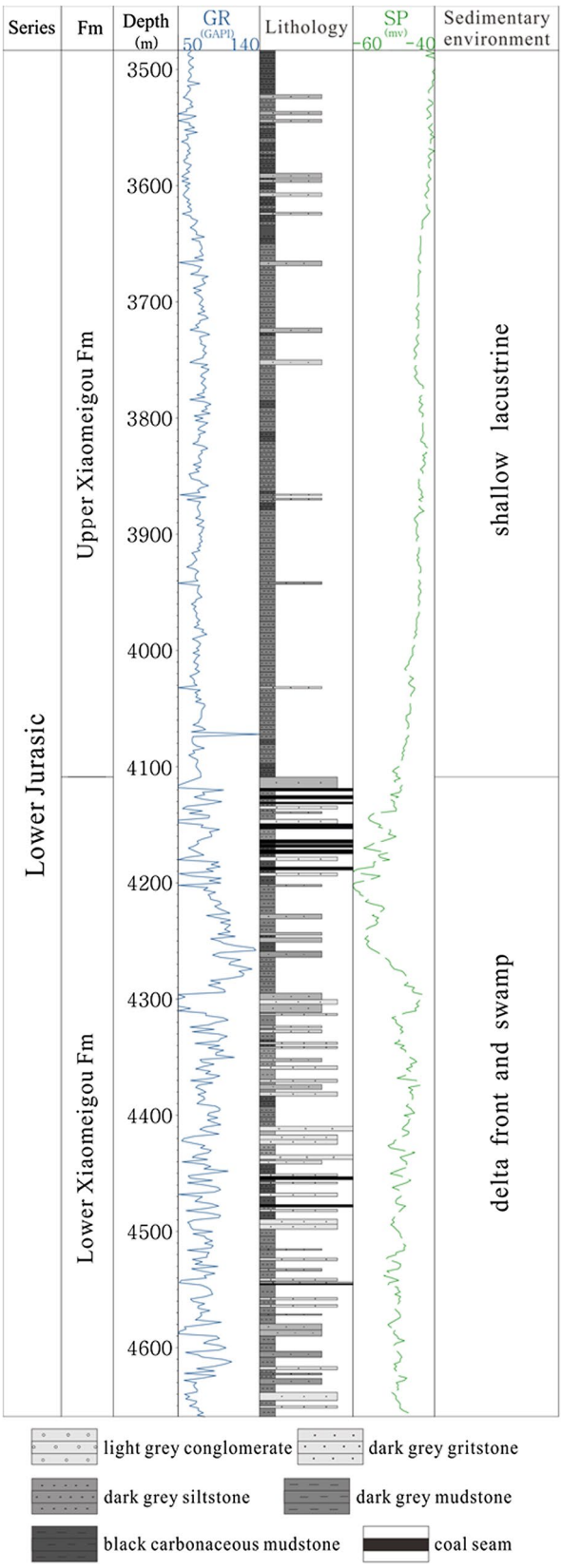


**Fig. 2** The sedimentological and petrophysical characteristics of lower Jurassic of LK1 in north Margin of Qaidam Basin

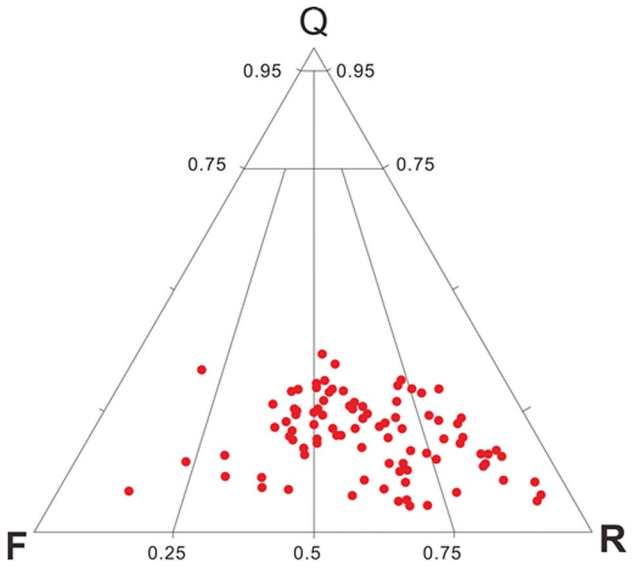


**Fig. 3** Triangle diagram of lower Jurassic sandstone components in the Lenghu V tectonic belt

by microcline. The rock fragments are mainly metamorphic rocks, followed by magmatic rocks. The size of grains is fine–medium and sorting is poor–medium. The pore fillings are dominated by clay minerals, followed by carbonate and siliceous cements. The mineralogical and textural maturities are low.

Generally, detrital kaolinite is abundant in the humid tropics and subtropics (Tang et al. 2002; Zeng and Xia 1986), and an increase in detrital chlorite and illite content indicates an arid climate (Chamley 1989; Perederij 2001).

According to X-ray diffraction data (Table 1), the clay mineral assemblage of mudstone in the Xiaomeigou Fm is illite + kaolinite + illite/smectite (K + I + I/S), and the mixed-layer ratio (S%) of I/S is 8–25%. The relative content of clay minerals shows general abnormal high kaolinite content (40–66%, average 48%). Although some kaolinite must be generated from digenetic process, the majority of kaolinite in the mudstone is definitely from terrigenous clastic materials, for example, the clay mineral assemblage I + K could represent a humid climate (Yuan et al. 2007). Furthermore, kaolinite contents of the Xiaomeigou Fm ($J_1$) and the overlying Lulehe Formation ($E_{1+2}$) have significant difference, which indicates that at least part of the kaolinite is detrital (Austin 1970, 1971).

## Carbon and oxygen isotopes

### Results

The carbon and oxygen isotope data of 34 samples are shown in Table 2. The $\delta^{18}O$ values range from − 18.523‰ to − 8.344‰ with an average of − 13.31‰. The $\delta^{13}C$

**Table 1** X-ray diffraction analysis of the lower Jurassic mudstone in the Lenghu V tectonic belt

| Depth/m | Formation | Lithology | Relative content in clay minerals(%) | | | | | | Mixed-layer ratio(S%) | |
|---|---|---|---|---|---|---|---|---|---|---|
| | | | S | I/S | I | K | C | C/S | I/S | C/S |
| 2800.00 | $E_{1+2}$ | Mudstone | \ | 40 | 34 | \ | 26 | \ | 35 | \ |
| 2900.00 | $E_{1+2}$ | Mudstone | \ | 33 | 43 | \ | 24 | \ | 35 | \ |
| 3000.00 | $E_{1+2}$ | Mudstone | \ | 20 | 60 | \ | 20 | \ | 40 | \ |
| 3200.00 | $E_{1+2}$ | Mudstone | \ | 21 | 64 | 4 | 11 | \ | 40 | \ |
| 3482.25 | $J_1$ | Mudstone | \ | 3 | 31 | 66 | \ | \ | 8 | \ |
| 3720.00 | $J_1$ | Mudstone | \ | 23 | 17 | 46 | 14 | \ | 25 | \ |
| 3840.00 | $J_1$ | Mudstone | \ | 15 | 25 | 46 | 14 | \ | 25 | \ |
| 4060.00 | $J_1$ | Mudstone | \ | 14 | 26 | 47 | 13 | \ | 25 | \ |
| 4120.00 | $J_1$ | Mudstone | \ | 7 | 32 | 50 | 11 | \ | 25 | \ |
| 4280.00 | $J_1$ | Mudstone | \ | 25 | 23 | 41 | 11 | \ | 20 | \ |
| 4309.95 | $J_1$ | Mudstone | \ | 48 | 11 | 41 | \ | \ | 20 | \ |
| 4311.63 | $J_1$ | Mudstone | \ | 13 | 35 | 52 | \ | \ | 11 | \ |
| 4321.36 | $J_1$ | Mudstone | \ | 20 | 27 | 40 | 13 | \ | 20 | \ |
| 4381.10 | $J_1$ | Mudstone | \ | 5 | 22 | 61 | 12 | \ | 20 | \ |
| 4417.81 | $J_1$ | Mudstone | \ | 14 | 27 | 47 | 12 | \ | 20 | \ |

Standard: SY/T 5163-1995. The reason that S + I/S + I +K +C + C/S = 101 or 99 is rounded numbers rather than data bias. Clay mineral with mixed-layer ratio greater than 70% is smectite. Where S is smectite, I/S is illite/smectite mixed-layer, I is illite, K is kaolinite, C is chlorite, and C/S is chlorite/smectite mixed-layer. Mixed-layer ratio, 20% for example, means the ratio between illite and smectite or chlorite and smectite is 20

**Table 2** The carbon–oxygen isotopic composition of the lower Jurassic clastic rocks from the Lenghu V tectonic belt

| Well | Depth/m | Lithology | Major cement | $^{13}C$/‰ | $^{18}O$/‰ | Temperature/ °C | *Z* |
|---|---|---|---|---|---|---|---|
| LK1 | 3482.10 | Light gray grit | Ferrocalcite | − 11.18 | − 13.68 | 95.55 | 97.60 |
| LK1 | 3483.50 | Gray siltstone | Calcite | − 6.08 | − 10.61 | 74.63 | 109.56 |
| LK1 | 3486.13 | Gray siltstone | Ferrocalcite | 4.10 | − 13.42 | 93.68 | 129.01 |
| LK1 | 3512.45 | Gray siltstone | Ferrocalcite | 4.94 | − 10.74 | 75.50 | 132.07 |
| LK1 | 3514.40 | Gray fine sandstone | Ferrocalcite | 5.74 | − 8.34 | 60.41 | 134.90 |
| LK1 | 3516.45 | Gray fine sandstone | Siderite | 4.01 | − 8.60 | 61.96 | 131.22 |
| LK1 | 3518.40 | Gray siltstone | Ferrocalcite | 3.83 | − 11.44 | 80.11 | 129.44 |
| LK1 | 3519.80 | Gray siltstone | Siderite | 4.44 | − 8.59 | 61.92 | 132.11 |
| LK1 | 3538.10 | Gray siltstone | Ferrocalcite | 5.75 | − 13.01 | 90.78 | 132.60 |
| LK1 | 3540.15 | Gray siltstone | Siderite | 4.55 | − 11.57 | 80.98 | 130.86 |
| LK1 | 3542.20 | Gray siltstone | Ferrocalcite | 6.63 | − 9.44 | 67.15 | 136.18 |
| LK1 | 3542.55 | Gray siltstone | Ferrocalcite | 6.50 | − 9.86 | 69.78 | 135.70 |
| LK1 | 3753.20 | Gray fine sandstone | Ferrocalcite | − 5.22 | − 18.01 | 128.24 | 107.63 |
| LK1 | 3755.60 | Gray siltstone | Ferrocalcite | 6.68 | − 9.69 | 68.73 | 136.16 |
| LK1 | 3755.90 | Gray siltstone | Ferrocalcite | 9.21 | − 8.58 | 61.86 | 141.88 |
| LK1 | 4235.10 | Gray siltstone | Ferrocalcite | − 0.02 | − 16.59 | 117.06 | 118.99 |
| LK1 | 4239.30 | Gray fine sandstone | Calcite | − 1.70 | − 13.13 | 91.64 | 117.27 |
| LK1 | 4306.30 | Gray fine sandstone | Ferrocalcite | − 10.64 | − 16.30 | 114.88 | 97.39 |
| LK1 | 4307.40 | Gray fine sandstone | Ferrocalcite | − 10.71 | − 16.51 | 116.50 | 97.15 |
| LK1 | 4308.20 | Gray coarse sandstone | Ferrocalcite | − 11.44 | − 16.71 | 117.99 | 95.55 |
| LK1 | 4310.60 | Gray fine sandstone | Ferrocalcite | − 9.35 | − 16.18 | 113.94 | 100.09 |
| LK1 | 4312.00 | Gray fine sandstone | Calcite | − 5.00 | − 14.99 | 105.00 | 109.59 |
| LK1 | 4313.20 | Gray coarse sandstone | Ferrocalcite | − 11.94 | − 18.52 | 132.34 | 93.62 |
| LK1 | 4314.70 | Pebbly medium–fine sandstone | Ferrocalcite | − 11.3 | − 18.20 | 129.70 | 95.09 |
| LK1 | 4316.20 | Gray medium sandstone | Ferrocalcite | − 6.56 | − 15.67 | 110.05 | 106.06 |
| LK1 | 4318.00 | Gray fine sandstone | Ferrocalcite | − 11.42 | − 16.57 | 116.91 | 95.65 |
| LK1 | 4320.80 | Coarse sandstone | Ferrocalcite | − 3.39 | − 16.85 | 119.08 | 111.97 |
| LK1 | 4377.50 | Gray fine sandstone | Ankerite | − 1.51 | − 12.79 | 89.24 | 117.85 |
| LK1 | 4379.50 | Gray coarse sandstone | Ferrocalcite | − 7.12 | − 16.48 | 116.27 | 104.51 |
| LK1 | 4381.30 | Gray medium–fine sandstone | Ferrocalcite | − 6.31 | − 13.81 | 96.49 | 107.49 |
| LK1 | 4384.10 | Gray fine sandstone | Ferrocalcite | − 5.05 | − 14.23 | 99.46 | 109.87 |
| LK1 | 4413.80 | Gray coarse sandstone | Ferrocalcite | − 15.57 | − 12.95 | 90.41 | 88.95 |
| LK1 | 4417.00 | Gray medium–fine sandstone | Ferrocalcite | − 10.13 | − 14.08 | 98.36 | 99.55 |
| LK1 | 4418.56 | Pebbly coarse sandstone | Ferrocalcite | − 12.39 | − 15.26 | 106.99 | 94.34 |

values range from − 15.574‰ to 9.207‰ with an average of − 3.16‰.

## Sedimentary environment analysis

In general, carbon and oxygen isotopes of carbonate cements are controlled by two factors. One is the sedimentary environment (paleosalinity) where the cements were initially precipitated in the eodiagenesis; the other one is a later diagenetic phase (Wang et al. 2010; Wei et al. 2015).

There are two carbon pools, inorganic and organic. The $\delta^{13}C$ values of inorganic carbon range from − 4.0‰ to 4.0‰, while organic carbon $\delta^{13}C$ always has negative bias (Wang et al. 2007). The $\delta^{13}C$ of native carbonate rocks in lacustrine facies range from − 6.0‰ to − 2.0‰ (Kelts and Talbot 1990). Under certain salinities, oxygen isotopes of carbonate cements would have a negative bias with increasing temperature.

However, $\delta^{13}C$ and $\delta^{18}O$ have a positive bias if the salinity increased (Liu et al. 2006a). Keith and Weber (1964) summarized the connection between the two values and put forward an empirical coefficient *Z* ($Z = 2.048 \times (\delta^{13}C + 50) + 0.498 \times (\delta^{18}O + 50)$) to distinguish marine limestone ($Z > 120$) from freshwater limestone ($Z < 120$). This method is more effective for carbonate cements less affected by diagenesis (Cerling 1984; 1991; Driese and Mora 1993).

Isotopic data from this test are related to bulk sample and mainly related to carbonate cements and phases. The samples with negative biases in $\delta^{18}O$ (< 14‰) and $\delta^{13}C$ values indicate that they formed in mesodiagenesis which was strongly affected by organic carbon. For samples with higher $\delta^{18}O$ values (> 14‰), most of them have positive bias in $\delta^{13}C$ values($\delta^{13}C > 4‰$, $Z > 120$) except for one sample (Fig. 4; Table 2). This positive bias was caused by methanogenesis. More details are discussed in discussion part. So, if the samples affected by diagenesis are removed, the rest of the samples reflect the fresh water environment ($\delta^{13}C = -1.70‰$, $\delta^{18}O = -13.13‰$, $Z = 117.27$; $\delta^{13}C = -1.51‰$, $\delta^{18}O = -12.79‰$, $Z = 117.85$; $\delta^{13}C = -6.08‰$, $\delta^{18}O = -10.61‰$, $Z = 109.56$). And, the later period may be warmer and wetter in Early Jurassic.

## Elemental geochemistry characteristics

### Major elements

In different sedimentary environments, different elements have varying characteristics regarding dissolution, migration and enrichment. Thus, the analysis of elemental content can provide information on the paleoenvironment (Xiong and Xiao 2011; Wang et al. 2006). The major elements of bulk samples could be characterized as mixtures of terrigenous–detrital matters comparable to average shale with varying amounts of calcium carbonate. Compared to the average shale (Gromet 1984), the major elements in the Xiaomeigou Fm generally show high $Al_2O_3$ and low CaO, $K_2O$, $Na_2O$ and MgO contents (Fig. 5) (Sun et al. 2015a). The relatively

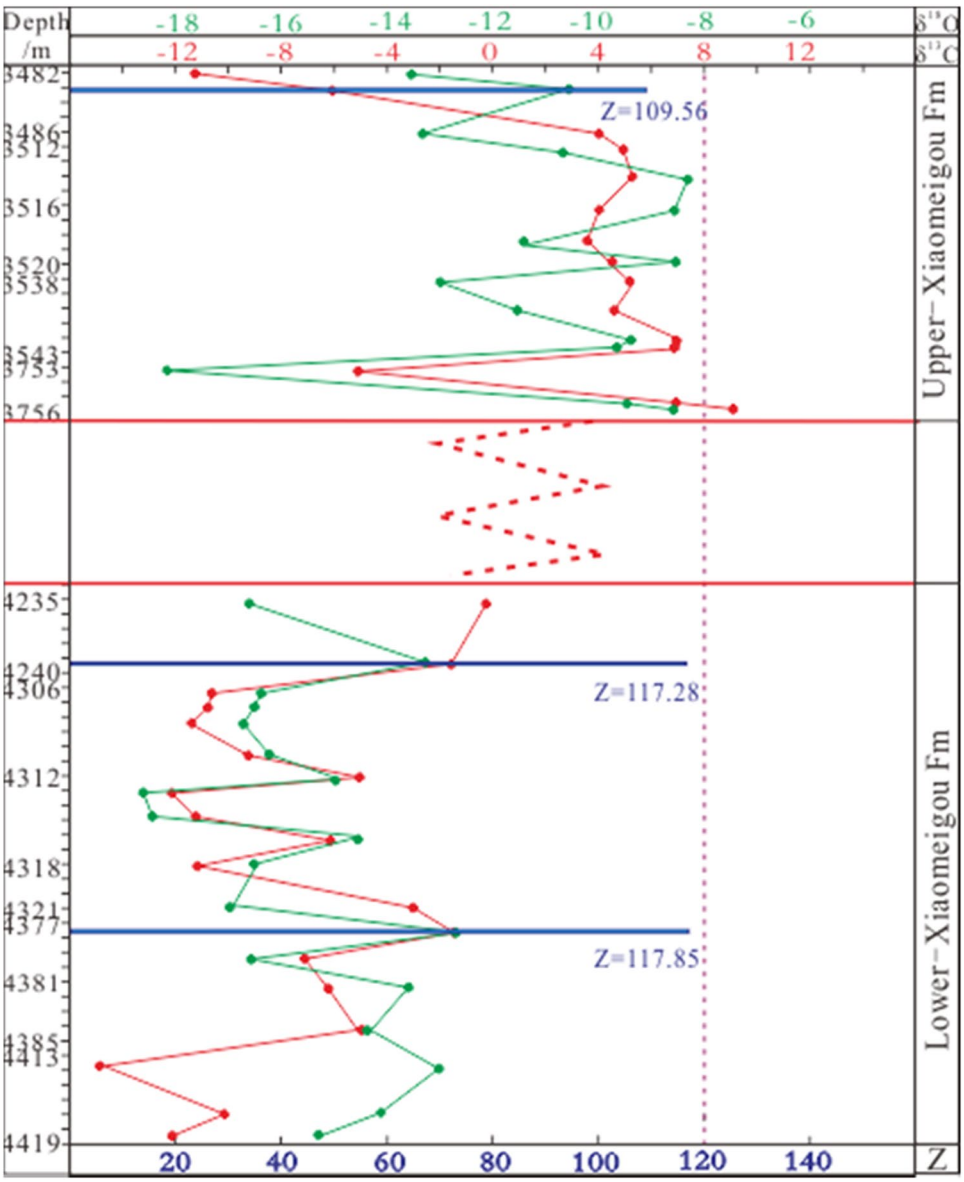


**Fig. 4** The *Z* value and carbon–oxygen isotope tracks of the Xiaomeigou Fm in the Lenghu V tectonic belt

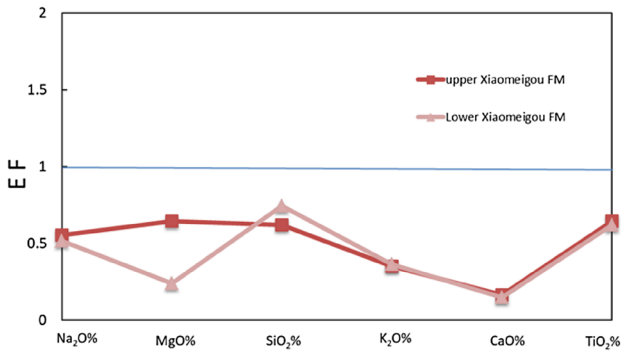


**Fig. 5** Comparison of major elements between samples and the average shale. EF (enrichment factor) = $C_{\text{sediment}}/C_{\text{standard rock}}$

**Table 3** correlation-coefficients(r) for selected major and minor elements with $p < 0.01$

| | *r* | | *r* | | *r* |
|---|---|---|---|---|---|
| $Al_2O_3$-$K_2O$ | 0.817 | $K_2O$-$TiO_2$ | 0.803 | $K_2O$-Rb | 0.930 |
| $Al_2O_3$-$TiO_2$ | 0.801 | $Al_2O_3$-Rb | 0.879 | $TiO_2$-Rb | 0.816 |

low content of easily dissolved elements like Ca, Mg and Na suggests that the evaporation was weak in early Jurassic (Fig. 5). According to the analytical results, $Al_2O_3$, $K_2O$, $TiO_2$ and Rb have strong positive correlations (Table 3), and this could indicate a dominated terrigenous–detrital origin of these elements (Hild and Brumsack 1998).

There is an obvious decrease from the bottom to the top Xiaomeigou Fm in elements from detrital input like Si, Al and K (Fig. 6).

## Trace elements

Variations in the concentration of trace elements may be controlled by their behaviors in the water column (conservative, coupled to biogenic cycles, etc.), redox conditions during deposition and the supply of terrigenous detrital material. Generally, trace elements are suspected to be mixed origin, that is, detrital and authigenic (Tribovillard et al. 2006).

As demonstrated above, the concentration of Rb could be greatly affected by detrital input, because of good correlations with $Al_2O_3$ ($r = 0.879$) and $TiO_2$ ($r = 0.816$) (Calvert and Pedersen 1993; Hild and Brumsack, 1998; B¨oning et al. 2004). Al-normalizing is used to avoid the influence of detrital input.

Redox-sensitive elements such as Cr, V can be fixed under reducing conditions, because its reduced state is more insoluble than oxic one (Calvert and Pedersen 1993). The upper Xiaomeigou Fm shows an enrichment in V and Cr (Figs. 7, 8).

Compared to average shale, Fe, Co and Mn are significantly enriched, especially in the upper Xiaomeigou Fm. They have significantly positive correlations with each other (Fe–Mn, $r = 0.886$; Fe-Co, $r = 0.958$; Mn-Co, $r = 0.875$). Also, they are negatively correlated with K, Rb, Al and Si(Fe–Al, $r = -0.829$; Fe–Si, $r = -0.884$),

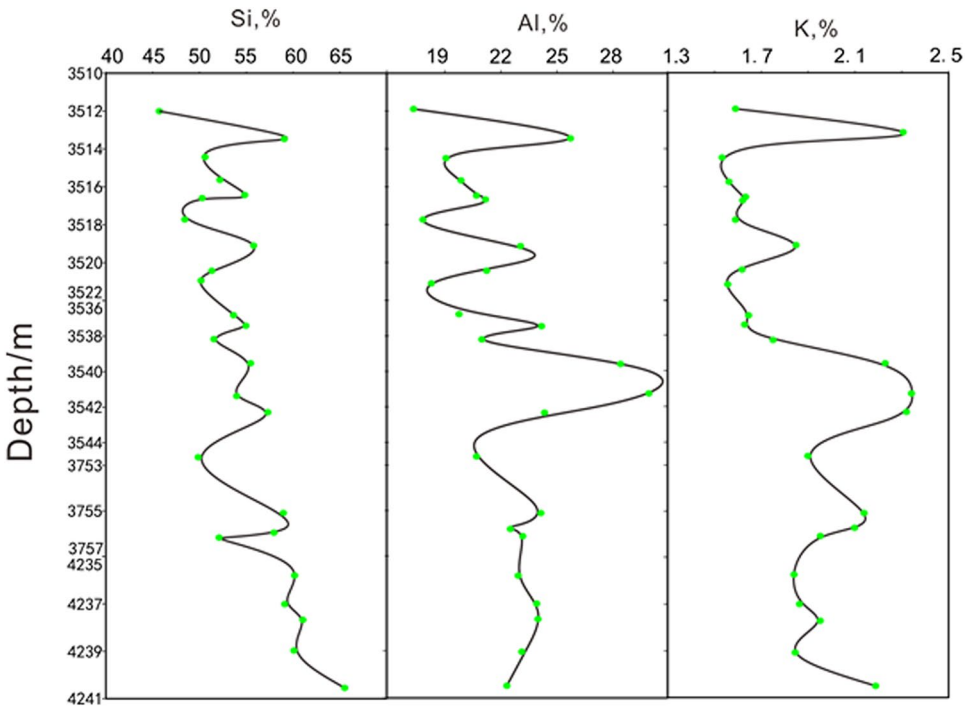


**Fig. 6** Depth profiles of Si, Al and K contents in core LK1

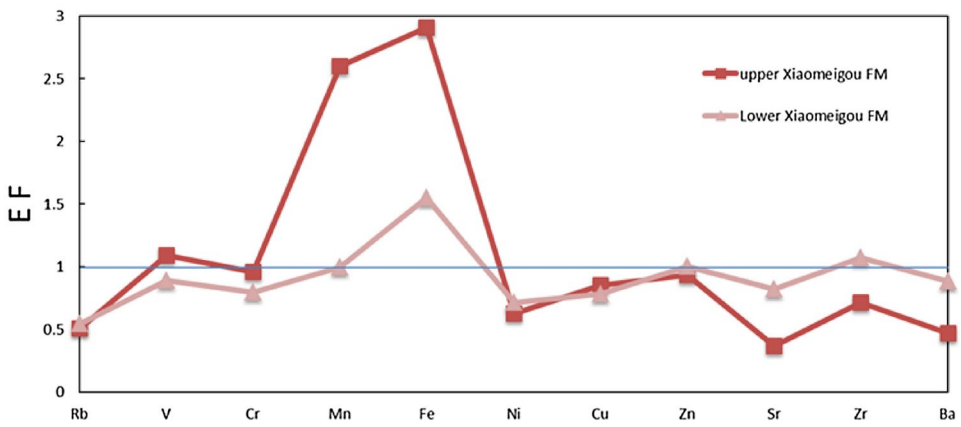


**Fig. 7** Comparison of trace elements between samples and the average shale. EF (enrichment factor) = $C_{\text{sediment}}/C_{\text{standard rock}}$

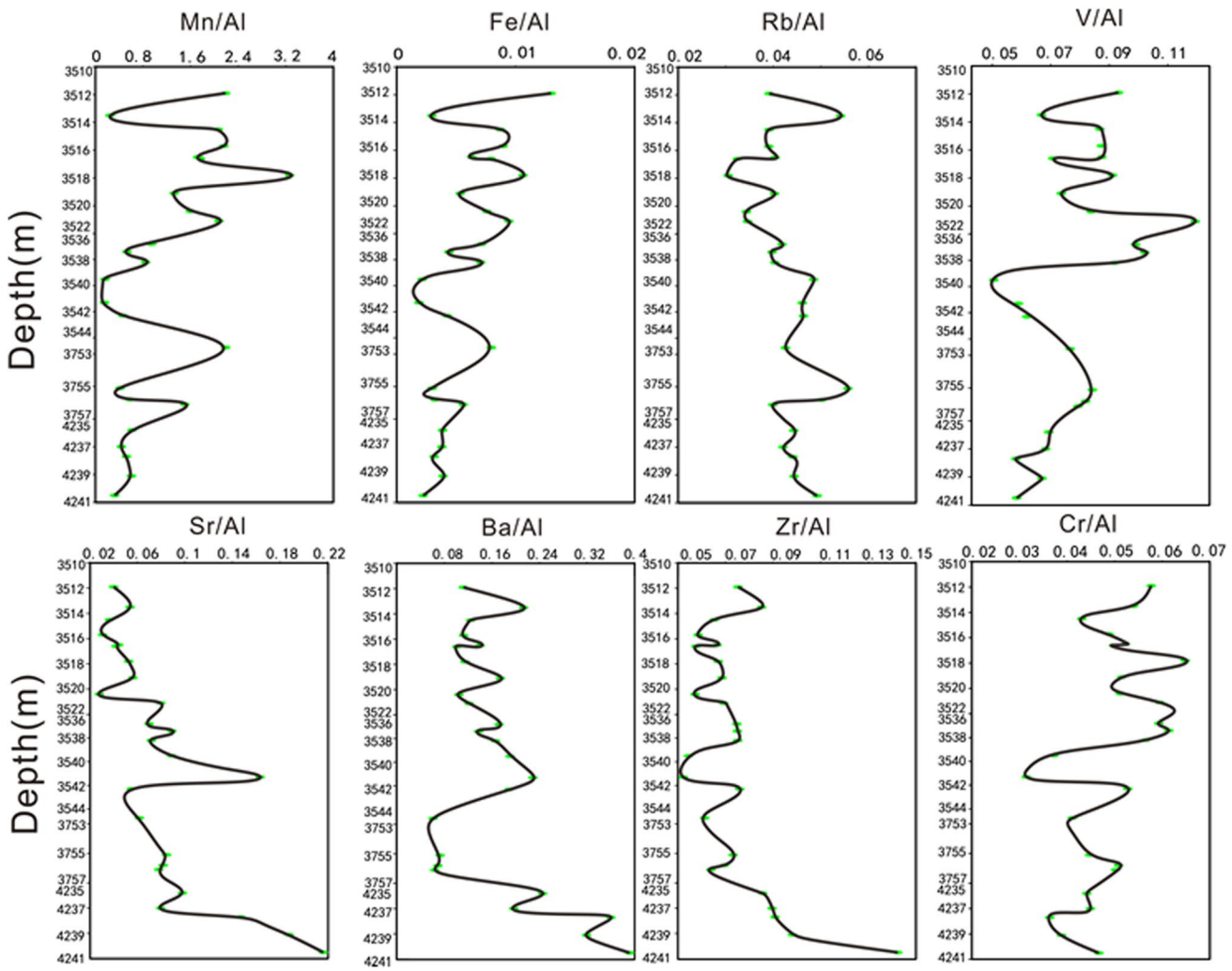


**Fig. 8** Depth profiles of selected trace element/Al ratios in core LK1. Trace element/Al ratios as weight-ratios

which suggests that they didn't originate from detrital matters, and they got enriched near the source. So, the increase in Fe, Mn and Co from the lower to the upper Xiaomeigou Fm (Fig. 8), together with decrease in K, Si and Al (Fig. 5), suggest expansion of the lake and rising of lake level.

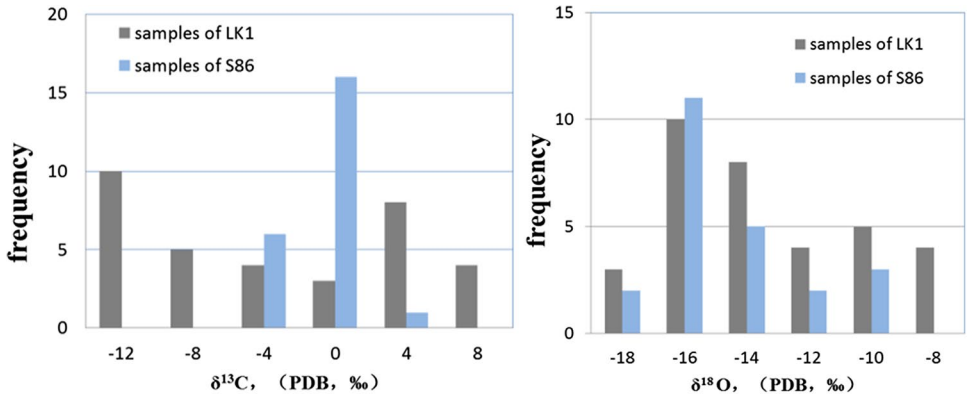


**Fig. 9** Histogram of carbon and oxygen isotopes of cores LK1 and S86

Sr and Ba obviously decreased from the lower to the upper Xiaomeigou Fm. They are positively well-correlated with each other (Sr–Ba, $r = 0.86$), indicating that they don't compete for anions and deposit in the form of bicarbonate in freshwater with lack of sulfate ion (Sun et al. 1997). They show a weakly positive correlation with K, Rb and Al (Sr–Al, $r = 0.616$; Ba–Al, $r = 0.642$). All of these demonstrate that the content of Sr and Ba are dominated by evaporation. However, detrital input contributed a little.

## Discussion

### Formation phases of carbonate cements

The sources and types of diagenetic fluid control the carbon isotope characteristics of carbonate cements, while the oxygen isotopes reflect the temperature and fluid component when the cements formed (Wang 2000).

The distribution pattern of carbon isotopes in the Xiaomeigou Fm is bimodal (Figs. 4, 10). One peak is − 12‰. It presents an obvious negative bias, which indicates that these cements are mainly formed in the mesodiagenesis (Surdam et al. 1984). This bias was caused by

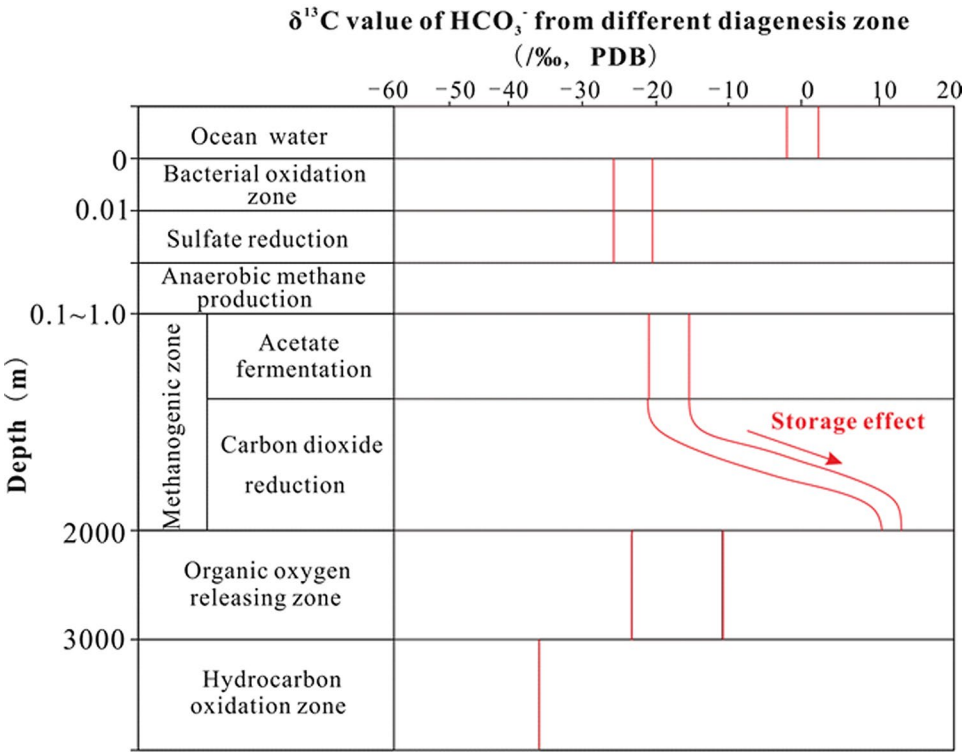


**Fig. 10** The carbon isotopic characteristics of bicarbonate of different sources (Irwin et al. 1977)

the $CO_2$ from decarboxylation of organic matters. The other peak is about 4‰, and these samples are only found in the upper Xiaomeigou Fm. This positive bias may be caused by arid climate or act of methanogens (Irwin et al. 1977). To distinguish between the influences of paleoenvironment and diagenesis, a comparison has been done with an additional well (S86).

The well S86 is located 17.5 km to the northwest of the LK1, and 23 sandstone samples from the Xiaomeigou Fm were collected. The depth of the Xiaomeigou Fm in S86 is from 3025 m to 4460 m, which is similar to LK1. The $\delta^{13}C$ values from S86 are concentrated between − 5.7 and 3.5‰, and the absence of negative peak suggests that organic carbon from decarboxylation is less than LK1. The distribution of $\delta^{18}O$ values from S86 is similar to data from LK1, indicating that these two wells were in the same temperature and pressure field and their pore water have the same evolution characteristics. Because these two wells are close, the difference in carbon and oxygen isotopes fractionation controlled by paleosalinity should be small. So, the positive bias in $\delta^{13}C$ in the upper Xiaomeigou Fm is due to the act of methanogens (Fig. 9).

During diagenesis, the positive bias of $\delta^{13}C$ in carbonate cements occurs in the methanogenic zone (Irwin et al. 1977). Below the sulfate reduction zone, methanogens act in an anaerobic environment (Rice and Claypool 1981), the processes are below (Schoell 1980; Rice and Claypool 1981):

$CH_3COOH$—$CO_2 + CH_4$ (acetate fermentation)

$CO_2 + 4H_2$—$CH_4 + 2H_2O$ (reduction of $CO_2$)

In this zone, short chain fatty acids and anions (acetate) from bacterial action generate $CO_2$ with high $\delta^{13}C$ (Wang 2000). Specifically, in the first stage, the fermentation of acetic acid generates $CO_2$ with low $\delta^{13}C$ (− 30 to − 20‰), but as the reaction went on, $\delta^{13}C$ of $CO_2$ is finally approaching to the $\delta^{13}C$ of carboxyl (− 10 to − 5‰). During the reduction of $CO_2$, the $\delta^{13}C$ of $CH_4$ ranges from − 60 to − 25‰, and it is more negative than the $\delta^{13}C$ of early $CO_2$. This leads to the enrichment of $^{13}C$ in later $CO_2$, changing the $\delta^{13}C$ of $CO_2$ near to + 15‰ (Fig. 10).

Shackleton (1974) proposed an empirical formula to calculate ancient temperatures using oxygen isotopes:

$T = 16.9 - 4.38 \times (\delta C - \delta W) + 0.10 \times (\delta C - \delta W)^2$, where δC represents the $\delta^{18}O$ value of carbonate cements (PDB), and δW represents the $\delta^{18}O$ value of sea water (Standard Mean Ocean Water, SMOW). Since the $\delta^{18}O$ value of Jurassic lake water is unknown, δW is assumed to be the same as that of modern ocean; i.e., δW = 0 (Shao 1994).

Based on the carbon and oxygen isotopes of samples from the Xiaomeigou Fm in LK1, the formation temperatures of carbonate cements can be calculated. The temperature values range from 60.4 to 132.3 °C. This wide range shows a complex influence of diagenetic environment.

The $\delta^{13}C$–$\delta^{18}O$ results (Fig. 9a) were used to determine the carbon source of the carbonate cements (Wang 2000; Guo and Wang 1999).

It is apparent that the carbonate cements of most samples directly precipitated from paleowater (Fig. 12a) in the Xiaomeigou Fm have gone through two diagenetic processes when buried deeply (Fig. 11a). One is the function of methanogens, which causes the positive bias of $\delta^{13}C$ in ferrocalcite (Wang 2000) (Fig. 12a). This ferrocalcite shows low $\delta^{18}O$ values (average is − 10.27‰). Based on empirical formula, the calculated formation temperature of these cements is between 60.4 and 93.6 °C, and average is 72.7 °C (Table 2), which is consistent with the activity temperature of methanogens (Liu et al. 2006b). These demonstrate that cements

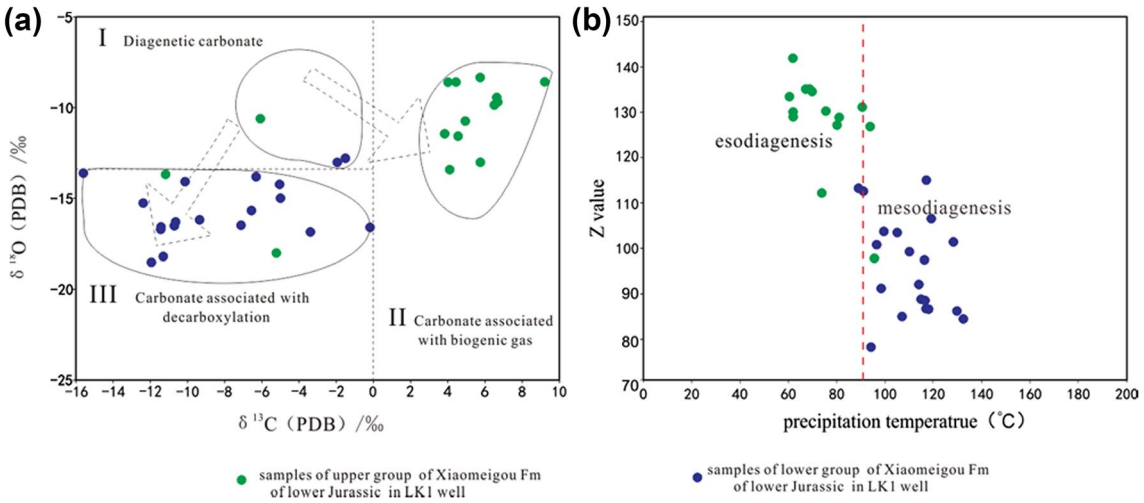


**Fig. 11** The carbonate cements of the lower Jurassic clastic rocks from the Lenghu V tectonic belt (Wang 2000; Guo and Wang 1999)

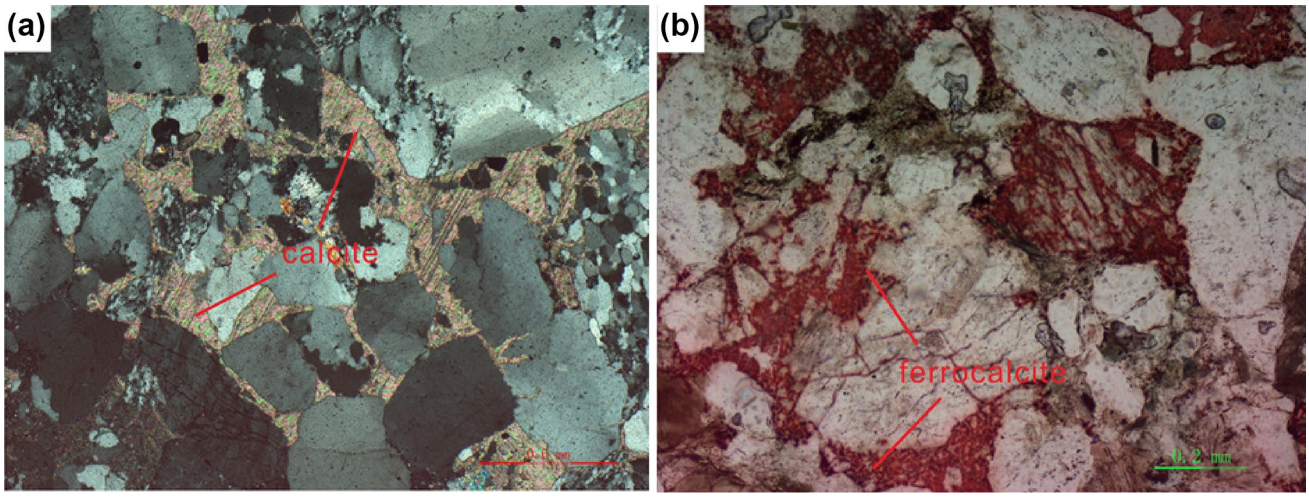


**Fig. 12** Microscopic photos of carbonate cements formed in different diagenesis stages. **a** 3483.5 m, LK1, calcite cements formed in esodiagenesis; **b** 4413.9 m, LK1, ferrocalcite formed in mesodiagenesis

with positive bias in carbon isotope formed in the late stage of eodiagenesis (< 90 °C) (Fig. 11b).

Another process is the decarboxylation of organic matters, leading to a negative bias of $\delta^{13}C$ in parts of ferrocalcite (Fig. 12b). These samples show very low $\delta^{18}O$ values (average is − 15.90‰), and the calculated temperature is between 90.4 and 132.3 °C, and average is 112.1 °C (Table 2). The result shows that the majority of the cements in these samples formed in mesodiagenesis (> 90 °C) (Surdam et al. 1989). When the hydrogen ions in the pore water are exhausted, the pore fluid characteristics change fundamentally. The dissolution of feldspar accumulates high cation concentrations. Thus, the pore fluid changed from acidic to alkaline, leading to the deposition of carbonate minerals include carbonate cements (Song et al. 2014). The diagenetic fluid is not entirely atmospheric-leaching water, and includes fluid generated from the evolution of organic matter.

## Sedimentary environments

### Paleosalinity

According to the analysis of isotopic data and the origins of carbonate cements, the cements of most samples in LK1 were affected strongly by the diagenesis. The effective data are with low $\delta^{18}O$ value and medium $\delta^{13}C$ value. Three samples in Lk1 (Table 2; Fig. 9b) demonstrate fresh water environment in early Jurassic (average *Z* value is 114).

Elemental chemistry has the same conclusion. Sr and Ba are less affected by detrital input. In lacustrine deposits, Sr/Ba > 1 always represents saline environment, whereas < 1 suggests fresh water (Wang 1996). Sr/Ba values in the Xiaomeigou Fm range from 0.25 to 0.71, which indicate that it was fresh water in early Jurassic. Sr/Ba values show a decreasing trend in the Xiaomeigou Fm (Fig. 13).

### Paleoclimate

As mentioned above, the relative low content of easily dissolved element like Ca, Mg and Na suggests that the evaporation was weak in early Jurassic.

Moreover, Sr/Ca, Sr/Cu, Mg/Ca are sensitive to the climate changes (Xiong and Xiao 2011; Liang et al. 2015; Wang et al. 1997). High values of Mg/Ca and Sr/Ca always correspond to dry and hot climate. It is humid climate when Sr/Cu < 10 (Xiong and Xiao 2011). Sr/Cu values range from 1.47 to 10.35 in the Xiaomeigou Fm, indicating that it was wet and warm in early Jurassic. All these ratios show a decreasing trend from bottom to top in the Xiaomeigou Fm, indicating a gradually warmer environment (Fig. 13).

### Paleoredox

U, V, Cr, Cu, Zn are sensitive to the redox environment. U, V and Cr can accumulate under denitrifying (anoxic) conditions, whereas Ni, Co, Cu, Zn and Mo are enriched mainly under sulfate-reducing (euxinic) conditions alone (Tribovillard et al. 2006). V and Cr show an obvious increase from bottom to top in the Xiaomeigou Fm (Fig. 8). The values of element ratios have the same conclusion. (Hatch and Leventhal 1992) think that V/(V + Ni) < 0.6 represent oxic environment, and > 0.84 represent euxinic environment. The V/(V + Ni) values in the Xiaomeigou Fm range from 0.66 to 0.92, and gradually increase from bottom to top (Fig. 13). There is an enrichment of V and Cr only in the upper Xiaomeigou Fm, indicating that it was anoxic environment.

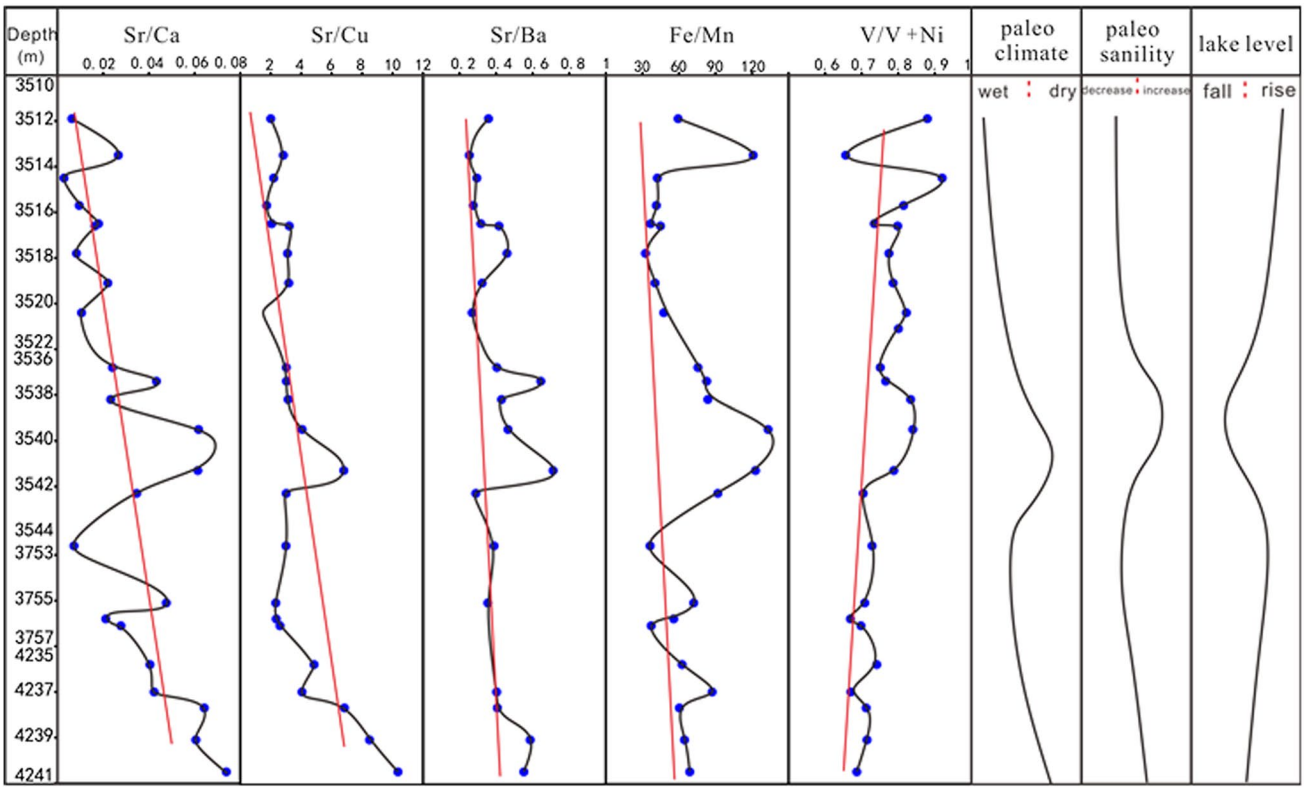


**Fig. 13** Variation of sedimentary environment in early Jurassic

It is consistent with the rising lake level. However, it was oxic–suboxic environment in the lower Xiaomeigou Fm.

## Conclusions

The strata of the Xiaomeigou Fm in LK1 are mainly dark gray or black mudstone with interbedded thin gray siltstone and greywacke layers. The high content of kaolinite in the Xiaomeigou Fm mudstone indicates a warm and wet climate.

The $\delta^{18}O$ value range from − 18.523 to − 8.344‰ (average is − 13.31‰) and the $\delta^{13}C$ value range from − 15.574 to 9.207‰ (average is − 3.16‰). Two diagenetic processes are distinguished in ferrocalcites. The first process is methanogenesis, which contribute to formation of ferrocalcites in temperatures from 60 to 90 °C. The ferrocalcites formed in temperatures from 90 to 140 °C were related to the decarboxylation of organic matter.

From the carbon and oxygen data of calcite cements ($Z < 120$) together with Sr/Ba values (Sr/Ba < 1), the fresh water environment can be concluded. And, paleosalinity tends to decrease from earlier to later Early Jurassic. The major element characteristics show that Al, K, Ti, Rb, Si are mainly from detrital matters. Sr, Ba, Fe, Mn, V and Cr are demonstrated to be less affected by detrital matters through relevance researches with Al. Sr and Ba are mainly controlled by evaporation. Sr/Cu and Sr/Ca ratios indicate that it was humid climate, and gradually became wetter and warmer during later early Jurassic. V/(V + Ni) values indicate it changed from oxic–suboxic environment to anoxic environment from lower to upper Jurassic.

**Acknowledgements** Contributions by Dr. Sun Guoqiang (Key Laboratory of Petroleum Resources, Gansu Province), in the development of this paper is greatly acknowledged. This study was supported by CAS "Light of West China" Program (Y304RC1SGQ).

## References

Austin G (1970) Weathering of the Sioux quartzite near New Ulm, Minnesota, as related to cretaceous climates. Sediment Petrol 40:184–193

Austin G (1971) Weathering of the Sioux quartzite near New Ulm, Minnesota, as related to Cretaceous climates-a reply to comment by D. M. Triplehorn. Sediment Petrol 40:604–605

B¨oning P, Brumsack HJ, B¨ottcher ME, Schnetger B, Kriete C, Kallmeyer J, Borchers SL (2004) Geochemis try of Peruvian near-surface sediments. Geochim Cosmochim Acta 68:4429–4451

Calvert SE, Pedersen TF (1993) Geochemistry of recent oxic and anoxic sediments: implications for the geological record. Mar Geol 113:67–88

Cerling TE (1984) The stable isotopic composition of modern soil carbonate and its relationship to climate. Earth Planet Sci Lett 71:229–240

Cerling TE (1991) Carbon dioxide in the paleoatmosphere: evidence from Cenozoic and Mesozoic paleosols. Am J Sci 291(4):377–400

Chamley H (1989) Clay sedimentology. Springer-Verlag, Heidelberg

Driese SG, Mora CL (1993) Physico-chemical environment of carbonate formation, Devonian vertic palaeosols, central Appalachians, USA. Sedimentology 40:199–216

Gromet LP (1984) The "North American shale composite": its compilation, major and trace element characteristics. Geochim Cosmochim Acta 48:2469–2482

Guo HL, Wang DR (1999) Stable isotopic composition and origin analysis of the carbonate cements with sandstone reservoir of Tarim oil-gas bearing area. Pet Explor Dev 26(3):31–34

Hatch JR, Leventhal JS (1992) Relationship between inferred redox potential of the depositional environment and the geochemistry of the Upper Pennsylvanian Stark Shale Member of the Dennis Limestone, Wabaunsee County, Kansas, USA. Chem Geol 99(1/3):65–82

Hild E, Brum sack HJ (1998) Major and minor element geochemistry of lower Aptian sediments from the NW German Basin (core Hoheneggelsen KB 40). Cretac Res 19:615–633

Hu ZQ (2003) Calcite cements in upper palaeozoic sand reservoir of Ordos Basin. Acta Pet Sinica 23(4):40–43 **(in Chinese with English abstract)**

Irwin H, Curtis C, Coleman M (1977) Isotopic evidence for source of digenetic carbonates formed during burial of organic-rich sediments. Nature 269(5625):209–212

Keith ML, Weber JN (1964) Isotopic composition and environmental classification of selected limestones and fossils. Geochim Cosmochim Acta 23:1786–1816

Kelts K, Talbot MR (1990) Lacustrine carbonates as geochemical archives of environment al change and biotic/abiotic interactions. In: Tilzer MM, Ser-ruya C (eds) Ecological structure and function in large lakes. Wis Science Tech, Madison, pp 290–317

Kou FD, Zhu YJ, Li JM (2005) The diagenesis of Lower Jurassic reservoir in Lenghu tectonic belt. J Oil Gas Technol 27(6):695–698

Liang WJ, Xiao CT, Xiao K, Lin W (2015) The relationship of Late Jurassic paleoenvironment paleoclimate with geochemical elements in Amdo Country of northern Tibet. Geol Chin 2(4):1079–1091

Liu CM, Li YL, Qi BW (2006a) Research status and exploration potential of biogenic gas. J Palaeogeogr 8(3):317–330

Liu DL, Sun XR, Li ZS, Tang NA, Tan Y, Liu B (2006b) Analysis of carbon and oxygen isotope on the Ordovician dolostones in the Ordos Basin [J]. Pet Geol Exp 28(2):155–161

Lu TQ, Ma ZQ, Mou ZH (1997) Jurassic system in Qaidam Basin of Qing Hai, China. Pet Exp Dev 24(6):17–20

Ma LX, Zhang M (2005) The recognition of lower Jurassic in LK1 in Qaidam Basin

Perederij VI (2001) Clay mineral composition and palaeoclimatic interpretation of the Pleistocene deposits of Ukraine. Quatern Int 76(77):113–121

Rice DD, Claypool GE (1981) Generation, accumulation, and resource potential of biogenic gas. AAPG Bull 65(1):5–25

Schoell M (1980) The hydrogen and carbon isotopic composition of methane from natural gases of various origins. Geochim et Cosmochim Acta 44(5):649–661

Shackleton NJ (1974) Attainment of isotopic equilibrium between ocean water and benthonic foraminifera genus Uvigerina: isotopic changes in the ocean during the last glacial Colloq. Int C N R S 1974(219):203–209

Shao YL (1994) The relation of the oxygen and carbon isotope in the carbonate rocks to the paleotemperature etc. J Chin Univ Min Technol 23(1):39–45

Song TS, Liu L, Wang YJ, Liu N, Yu M (2014) Characteristics and genesis of the bleached sandstone in, Ordos Basin. Oil Gas Geol 35(5):679–685

Sun ZC, Yang F, Zhang ZH et al (1997) Sedimentary environment and hydrocarbon generation of Cenozoic salinization lakes in China. Petroleum Industry Press, Beijing, pp 133–137

Sun GQ, Chen B, Zheng YX, Xie M, Xiao WM, Shi JA (2015a) Diagenesis and sedimentary environment of Miocene in Lenghu V tectonic belt. Nat Gas Geosci 26(4):679–688

Sun GQ, Yin JG, Zhang SC, Lu XC, Zhang SY, Shi JA (2015b) Diagenesis and sedimentary environment of Miocene series in Eboliang III area. Environ Earth Sci 74(6):5169–7159

Surdam RC, Boese SW, Crossey LJ (1984) The chemistry of secondary porosity. Aapg Memoir 37(2):183–200

Surdam RC, Crossey LJ, Hagen ES, Heasler HP (1989) Organic inorganic interactions and sandstone diagenesis. AAPG Bull 73:1–23

Tang YJ, Jia JY, Xie XD (2002) Environment significance of clay minerals. Earth Sci Front 9(2):337–341

Tribovillard N, Algeo TJ, Lyons T, Riboulleau A (2006) Trace metals as paleoredox and paleoproductivity proxies: an update. Chem Geol 232:12–32

Wang AH (1996) Discriminant effect of sedimentary environment by the Sr/Ba ratio of different existing forms. Acta Sedimentol Sin 14(4):168–173

Wang DR (2000) Stable isotope geochemistry of oil and gas. Petroleum Industry Press, Beijing, pp 82–85

Wang FQ, Wang BQ (2006) Diagenesis of reservoir rocks of the lower Jurassic and its influence on porosity modification in North Qaidam Basin. J Lanzhou Univ. 42(5):1–6

Wang SJ, Huang XZ, Tuo JC, Shao HS, Yan CF, Wang SQ, He ZR (1997) Evolutional characteristics and their paleoclimate significance of trace elements in the Hetaoyuan formation, Biyang depression. Acta Sedimentol Sin 15(1):65–70

Wang MF, Huang CY, Xu ZC, Chen JX, Yang S (2006) Review on paleosalinity recovery in sedimentary environment. Xinjiang Oil Gas 2(1):9–13

Wang Q, Zhuo XZ, Chen GJ, Li XY (2007) Characteristics of carbon and oxygen isotopic compositions of carbonate cements in Triassic Yanchang sandstone in Ordos Basin. Nat Gas Ind 27(10):28–32

Wang Q, Hao LW, Chen GJ, Zhang GC, Zhang R, Ma XF, Wang H (2010) Forming mechanism of carbonate cements in siliciclastic sandstone of zhuhai formation in baiyun sag. Acta Pet Sinica 31(4):553–558

Wei W, Zhu XM, Guo DB, Fei LY, Su H, Jiang FH (2015) Carbonate cements in lower cretaceous bayingebi sandstone reservoirs in Chagan Sag, Yin-e Basin: formation phases and formation mechanisms. Geochimica 44(6):590–599

Xie Y, Wang J, Li LX, Xie ZW, Deng GS, Li MH, Jiang XS (2010) Distribution of the Cretaceous clay minerals in Ordos basin, China and its implication to sedimentary and diagenetic environment. Geol Bull Chin 29(1):93–104

Xiong XH, Xiao JF (2011) Geochemical indicators of sedimentary environments-a summary. Earth Environ 39(3):405–413

Yang P, Yang YQ, Ma LX, Dong L, Yuan XJ (2007) Evolution of the Jurassic sedimentary environment in northern margin of Qaidam Basin and its significance in petroleum geology. Pet Exp Dev 34(2):160–164

Yuan Z, Li WH (2011) Origin of calcite cement in the sandstone reservoirs of the upper Triassic Yanchang Formation in Southeast of Ordos Basin. J Jilin Univ 41(1):17–23

Yuan HR, Nie Z, Liu JY, Wang M (2007) paleogene sedimentary characteristics and their paleoclimatic implications in Baise Basin. Guangxi J Palaeogeogr 81(12):1692–1697

Zeng YF, Xia WJ (1986) Sedimentary petrology. Petroleum Industry Press, Beijing, pp 125–142